

1 **This article has been published in the *Journal of Ecology*, please cite it as follows**

2 Deschamps, L., Maire, V., Chen, L., Fortier, D., Gauthier, G., Morneau, A., Hardy-
3 Lachance, E., Dalcher-Gosselin, I., Tanguay, F., Gignac, C., McKenzie, J. M., Rochefort,
4 L., & Lévesque, E. (2022). Increased nutrient availability speeds up permafrost
5 development, while goose grazing slows it down in a Canadian High Arctic wetland.
6 *Journal of Ecology*, 00, 1–15. <https://doi.org/10.1111/1365-2745.14037>

7

8 **The present version is the accepted manuscript before final editing.**

9

10

11 **Research paper**

12 **Title:** Increased nutrient availability speeds up permafrost development, while goose
13 grazing slows it down in a Canadian High Arctic wetland

14 **Authors:** Lucas Deschamps^{1,2,3*}, Vincent Maire^{1,2,3}, Lin Chen⁴, Daniel Fortier^{3,5}, Gilles
15 Gauthier^{3,6}, Amélie Morneau^{1,2}, Elisabeth Hardy-Lachance^{3,5}, Isabelle Dalcher-
16 Gosselin^{1,2}, François Tanguay^{1,2}, Charles Gignac^{3,7}, Jeffrey M. McKenzie⁸, Line
17 Rochefort^{3,7}, Esther Lévesque^{2,3}

18 **Address:**

19 1 Chaire en Écologie Fonctionnelle Arctique, Université du Québec à Trois-Rivières, Trois
20 Rivières, QC, G9A 5H7, Canada;

21 2 Département des sciences de l'environnement, Université du Québec à Trois-Rivières,
22 Trois Rivières, QC, G9A 5H7, Canada;

23 3 Centre d'études nordiques, Université Laval Québec, QC, G1V 0A6, Canada;

24 4 Department of Environmental Sciences, University of California, Riverside, CA 92521,
25 USA;

26 5 Département de géographie, Université de Montréal, Montréal, QC, H3T 1J4, Canada.

27 6 Département de biologie, Université Laval, QC, G1V 0A6, Canada

28 7 Département de Phytologie, Université Laval, Quebec City, QC, G1V 0A6, Canada

29 8 Department of Earth and Planetary Sciences, McGill University, Montréal, QC H3A 0E8,
30 Canada

31 *** Author for correspondence:**

32 **Lucas Deschamps**

33 Tel: +1 819 524-0245

34 Email: lucas.deschamps@uqtr.ca

35 **Word count:**

36 Total word count (excluding summary and legends): 8938

37 Summary: 332/350; Introduction: 1067; Materials and Methods: 1848; Results: 690;
38 Discussion: 2282; Acknowledgements: 159; References: 2892; Figures: 5; Tables: 3; No
39 of supporting Information files: 1

40 **Summary**

41 1) It is of prime importance to understand feedbacks due to the release of carbon (C)
42 stored in permafrost soils (permafrost-climate feedback) and direct impacts of
43 climatic variations on permafrost dynamics therefore received considerable
44 attention. However, indirect effects of global change, such as the variation in soil
45 nutrient availability and grazing pressure, can alter soil and surface properties of
46 the Arctic tundra, with the potential to modify soil heat transfers toward the
47 permafrost and impact resilience of Arctic ecosystems.

48 2) We determined the potential of nutrients availability and grazing to alter soil energy
49 balance using a 16-year split-plot experiment crossing fertilization at different
50 doses of nitrogen (N) and phosphorus (P) with protection from goose grazing. Moss
51 biomass and some determinants of the surface energy budget (leaf area index (LAI),
52 dead vascular plant biomass and albedo) were quantified and active layer thaw
53 depth repeatedly measured during three growing seasons. We measured soil
54 physical properties and thermal conductivity and used a physical model to link
55 topsoil organic accumulation processes to heat transfer.

56 3) Fertilization increased LAI and albedo, whereas grazing decreased dead vascular
57 plant biomass and albedo. Fertilization increased organic accumulation at the top
58 of the soil leading to drier and more porous topsoil, whereas grazing increased
59 water content of topsoil. As a result, topsoil thermal conductivity was higher in
60 grazed plots than in ungrazed ones. Including these properties into a simulation
61 model, we showed that, after 16 years, nutrient addition tended to shallow the
62 active layer whereas grazing deepened mean July active layer by 3.3 cm relative

63 to ungrazed subplots. As a result of OM accumulation at the surface, fertilization
64 increased permafrost vertical aggradation rate by almost an order of magnitude
65 (up to 5 mm·year⁻¹ instead of 0.7 mm·year⁻¹), whereas grazing slowed down
66 permafrost aggradation by reducing surface uprisings and deepening thaw depth.

67 4) *Synthesis*: We demonstrated that long-term grazing and N and P addition, through
68 their impact on vegetation and soil properties have the potential to impact
69 permafrost dynamics to the same extent as contemporary temperature increase in
70 High Arctic polygonal wetlands.

71 *KEYWORDS*: Active layer; Albedo; Fertilization; Global change ecology; Greater snow
72 goose; Organic matter; Polygons; Tundra

73

74

75 **Résumé**

76 **1)** Afin de comprendre les rétroactions causées par la respiration du carbone (C) stocké dans
77 le pergélisol (rétroaction pergélisol-climat), les impacts directs du changement climatique
78 sur la dynamique du pergélisol ont reçu une attention considérable. Toutefois, les effets
79 indirects du changement climatique, telles que la disponibilité en nutriments du sol et la
80 pression de broutement, peuvent altérer les propriétés du sol et de surface de la toundra
81 Arctique, avec le potentiel de modifier les transferts de chaleur vers le pergélisol et
82 d'impacter la résilience des écosystèmes Arctiques.

83 **2)** Nous avons déterminé l'effet potentiel d'une disponibilité accrue en nutriment et du
84 broutement sur la balance énergétique du sol grâce à une expérimentation en tiroir croisant
85 différents niveaux de fertilisation en azote (N) et phosphore (P) à une protection contre le
86 broutement durant 16 ans. La biomasse des plantes vasculaires et des mousses, ainsi que
87 plusieurs déterminants du budget radiatif de surface ont été quantifiés (indice de surface
88 foliaire (LAI), biomasse de plantes vasculaires mortes et albédo). La profondeur de la
89 couche active a été mesurée à répétition durant trois saisons de croissance. Les propriétés
90 physiques du sol et sa conductivité thermique ont été mesurées, et nous avons utilisé un
91 modèle physique de simulation pour lier l'accumulation de matière organique en surface
92 aux transferts de chaleur dans le sol.

93 **3)** L'indice de surface foliaire et l'albédo ont augmenté dans les traitements de fertilisation,
94 alors que le broutement a diminué la biomasse de plantes vasculaires mortes et l'albédo.
95 La fertilisation a causé l'ajout de nouveaux horizons organiques peu décomposés sous la
96 surface du sol, menant à des conditions plus sèches et à un sol plus poreux. À l'inverse, le
97 broutement a augmenté la teneur en eau du sol. En conséquence, la conductivité thermique
98 du sol était plus élevée dans les sous-parcelles broutées que dans celles non-broutées. En
99 incluant ces propriétés dans un modèle de simulation, nous avons montré que l'addition de

100 nutriments a diminué la profondeur de la couche active, tandis que le broutement l'a
101 approfondie de 3.3 cm en moyenne. En conséquence de la création de nouveaux horizons
102 organiques en surface, la fertilisation a augmenté le taux d'aggradation vertical du
103 pergélisol par un ordre de grandeur (jusqu'à $5.5 \text{ mm}\cdot\text{an}^{-1}$ au lieu de $0.7 \text{ mm}\cdot\text{an}^{-1}$), tandis
104 que le broutement a ralenti l'aggradation du pergélisol en limitant l'élévation de la surface
105 et en approfondissant la couche active.

106 **4) Synthèse** : Nous avons montré que l'effet à long-terme du broutement et de l'ajout de N et
107 P influençait la dynamique du pergélisol dans la même mesure que les augmentations de
108 températures contemporaines, et ce en impactant la végétation et les propriétés du sol dans
109 les marais polygonaux du Haut-Arctique.

110 **Introduction**

111 Thawing of the active layer (AL), the near-surface part of permafrost seasonally warming
112 above 0 °C, has important impacts on net carbon emission in the Arctic biome and may
113 turn it from a carbon sink to a carbon source (Schuur *et al.*, 2009; Koven *et al.*, 2011; Miner
114 *et al.*, 2022). Much effort has been devoted to understanding the response of the AL to
115 increased radiative forcing and air temperature, both with modelling (Schädel *et al.*, 2018)
116 and empirical (Hollister *et al.*, 2006) approaches. Physical properties of the land surface
117 influence transmission of radiation and energy partitioning among heat fluxes and may
118 slow or accelerate AL thaw rate and increase depth depending upon topsoil characteristics
119 and vegetation cover (Yi *et al.*, 2007). Surface properties are strongly influenced by
120 vegetation, for example through its influence on snow accumulation (Myers-Smith *et al.*,
121 2011) or shading (Blok *et al.*, 2010). Because Arctic vegetation is driven by indirect
122 influences of climate (for instance nutrient availability, Gough *et al.*, 2016; hydrology,
123 Hodkinson *et al.*, 1999) and other unrelated forces (for instance grazing, Pouliot *et al.*,
124 2009), global change may alter local AL dynamic in unexpected ways.

125 Nutrient availability may alter AL thaw through its impact on tundra vegetation. Nutrient
126 availability is expected to increase in terrestrial Arctic ecosystems following an increase of
127 topsoil temperature (Hartley *et al.*, 1999, Koven *et al.*, 2015). Arctic vegetation growth has
128 been demonstrated to be co-limited by N and P (Shaver & Chapin, 1995; Gough & Hobbie,
129 2003). Grasses (Liu *et al.*, 2020; Yläne *et al.*, 2020) and deciduous shrubs (Shaver *et al.*,
130 2001; van Wijk *et al.*, 2004; Gu & Grogan, 2020) benefit generally the most from increased
131 nutrient availability in topsoils, at the expense of mosses, which become submitted to
132 severe light limitation (Grellman, 2002; Gough *et al.*, 2016). The net effect of such

133 vegetation change on active layer depth is however not evident. An increase in dead
134 vascular plant and grass cover increases albedo (te Beest *et al.*, 2016), while an increase in
135 shrub cover and height diminishes it (Juszak *et al.*, 2014), decreasing and increasing the
136 quantity of energy available to warm the system, respectively. Higher vascular plant leaf
137 area index (LAI) reduces radiative input at the soil surface by shading (Juszak *et al.*, 2016
138 and 2017), potentially reducing the available energy to thaw the active layer (Blok *et al.*,
139 2010). The reduction in moss cover potentially removes an insulative layer at the top of the
140 soil column (Gornall *et al.*, 2009, Soudzilovskaia *et al.*, 2013) and can increase AL depth
141 (Gornall *et al.*, 2007). Altogether, these changes all represent potential vegetation-mediated
142 feedback between global warming and active layer depth, as nutrient availability is
143 expected to increase along with Arctic temperatures.

144 Grazing by abundant herbivore populations has the potential to increase thaw depth through
145 their impact on vegetation. Grazing generally reduces living vascular plant biomass
146 (Gauthier *et al.* 1995; Sjögersten *et al.*, 2011 for goose grazing, Falk *et al.*, 2015 for
147 mammal grazing; but see Bernes *et al.*, 2015 for reindeer grazing), potentially reducing
148 live LAI (Sundqvist *et al.*, 2019 for mammal grazing) and dead vascular plant accumulation
149 (Speed *et al.*, 2010; Sjögersten *et al.*, 2012 for goose grazing; Mosbacher *et al.*, 2019 for
150 mammal grazing). This results in an increase in the quantity of radiation reaching the
151 ground (Juszak *et al.*, 2016 and 2017). Conversely, reduction of shrub cover by heavy
152 mammalian grazing increases albedo, thereby decreasing the quantity of energy able to
153 thaw the active layer (te Beest *et al.*, 2016). Goose feeding on below-ground parts
154 (grubbing) is also known to disturb the moss mat, decreasing its insulative effect (van der
155 Wal *et al.*, 2001, Gornall *et al.*, 2009) with an unknown long-term effect on AL depth.

156 Arctic herbivores certainly have the potential to influence surface radiative transfer in
157 Arctic terrestrial ecosystems, but their impact in the context of increased soil nutrient
158 availability is poorly known.

159 Fertilization and grazing may affect active layer thaw through their impact on soil organic
160 matter (SOM) accumulation. Long-term SOM accumulation causes the extension of
161 syngenetic permafrost (the permafrost building upward after an addition of material at the
162 surface, Vincent *et al.*, 2017). Relative to mineral topsoil, low thermal diffusivity of SOM
163 at the top of the soil protects permafrost from thaw (Jorgenson *et al.*, 2010) and favors the
164 creation of a thick, ice-rich transient layer at the top of the permafrost table (Shur *et al.*,
165 2005). Both fertilization and grazing have the potential to alter SOM quantity and structure
166 by altering both the C fixation and decomposition rates in Arctic ecosystems. A long-term
167 Alaskan study revealed increased SOM accumulation in the first 5 cm, and a decreased of
168 SOM abundance below 5 cm in the soil of an experiment adding N and P simultaneously
169 (Mack *et al.*, 2004). There is evidence that while fertilization increases C input and storage
170 in the shallowest horizon, it may accelerate decomposition at depth (Nowinski *et al.*, 2008).
171 Both goose grazing (Sjögersten *et al.*, 2012) and grubbing (van der Wal *et al.*, 2007) have
172 been shown to reduce SOM stocks by reducing vascular plant growth and litter
173 accumulation at Svalbard. Topsoil water content (SWC) has also been shown to be
174 increased by goose grazing in Arctic wetlands (Sjögersten *et al.*, 2011 and 2012),
175 potentially increasing topsoil thermal conductivity (O'Donnell *et al.*, 2009). Both grazing
176 and increased nutrient availability may alter SOM accumulation at the top of the soil, but
177 the consequences for active layer thaw and permafrost development are still to be explored.

178 The aim of this study is to reveal the potential long-term effects of surface fertilization and
179 grazing by greater snow geese [*Anser caerulescens caerulescens* (Linnaeus, 1758)], an
180 important grazer of the tundra (Gauthier et al. 2006), on active layer thaw in polygonal
181 wetlands of a Canadian High Arctic oasis (Bylot Island, Nunavut). To do so, we
182 characterized vegetation, surface properties, hydrology, and soil thermal properties in a 16-
183 year-old experiment of fertilization and grazing exclusion. Our hypotheses are:

184 H1) N and P fertilization will increase leaf area index and dead vascular plant biomass, and
185 consequently increase surface albedo by covering the wet and dark moss layer, while grazing is
186 expected to reduce LAI, dead vascular plant biomass and albedo.

187 H2) N and P fertilization will increase organic matter accumulation at the top of the soil,
188 while grazing will limit such accumulation.

189 H3) N and P fertilization will decrease seasonal thaw depth, while grazing will increase it.

190

191 **Materials and methods**

192 **Site**

193 The experiment took place in the Qarlikturvik valley, on Bylot Island, Nunavut, Canada
194 (73°08'N, 80°00'W). The geomorphology of this glacial valley is characterized by a
195 succession of glacio-fluvial outwash, proglacial river, alluvial fans, and aggradation
196 terraces. The surface is almost continuously covered by vascular plants and mosses and
197 may be considered as a polar oasis (Bliss & Matveyeva, 1992). About 23% of the 70 km²
198 of the valley and surrounding upland is covered by wetlands located in low centered
199 polygons (Hughes *et al.*, 1994a) dominated by sedges (*Carex aquatilis* Walhenb.,
200 *Eriophorum angustifolium* Honck, *E. scheuzerii* Hoppe), grasses (*Dupontia fischeri* R.Br.,
201 *Pleuropogon sabinei* R.Br., Gauthier *et al.*, 1995) and mosses (*Drepanocladus* spp.,
202 *Calliergon giganteum* (Schimp.) Kindb., Pouliot *et al.*, 2009). Mesic environments occur
203 on polygonal rims, degraded and high centered polygons, in alluvial fans and in hummocky
204 tundra on the gentle slopes on either side of the valley (Zoltai *et al.*, 1983). Abundant
205 wetland vegetation allows the valley to be one of the most important brood-rearing sites
206 for the Greater Snow Goose in the Canadian Arctic with about 20,000 nesting pairs (Reed
207 *et al.*, 2002). Greater Snow Geese mostly feed on *D. fischeri* and *Eriophorum* spp. in
208 wetlands and are known to impact wetland vegetation biomass and nutrients concentration
209 (Gauthier *et al.*, 1995, Valéry *et al.*, 2010).

210 **Experimental design**

211 A long-term randomized block split-plot design with four block and four fertilization
212 treatments plus a control were established in polygonal wetlands of the valley in 2003.

213 Blocks were selected with a distance of at least 500 m from one another to capture polygon
214 heterogeneity in terms of vegetation, substrate type and soil wetness. Within polygons,
215 fertilization treatments were randomly attributed to five 2 m x 2 m permanent plots and
216 fertilized yearly between 2003 and 2019. Half of each plot (thereafter referenced as a
217 subplot) was protected with a permanent 50-cm tall chicken wire fence with ropes criss-
218 crossing the top since 2005, the protected part being randomly selected. During the
219 installation, plots were placed in homogeneous environment, characterized by a well-
220 developed moss-carpet and a good cover of graminoids typically grazed by geese. Plots
221 were at least 5 m apart to prevent cross-contamination of added nutrients (verified by
222 Pouliot *et al.*, 2009).

223 Fertilization treatments were selected to mimic both the range of potential nutrient release
224 associated with higher mineralization rates in the shallowest horizons of the soil (Gignac
225 *et al.*, 2022, Wang *et al.*, 2017), in addition to the possible nutrient addition via goose
226 faeces and atmospheric deposition. A low N treatment plot received $1 \text{ g}\cdot\text{m}^{-2}$ of N, whereas
227 the High N plot treatment received $5 \text{ g}\cdot\text{m}^{-2}$ of N. High P treatment was fertilized with 3
228 $\text{g}\cdot\text{m}^{-2}$ of P and the High N+P treatment with $5 \text{ g}\cdot\text{m}^{-2}$ of N and $1 \text{ g}\cdot\text{m}^{-2}$ of P. Control treatment
229 received the same quantity of water as other treatments. Fertilization treatments exceeded
230 the maximal amount of nutrients added by goose faeces (maximum of $29 \text{ faeces}\cdot\text{m}^{-2}$
231 recorded on a single plot, equivalent to $0.6\text{-}1 \text{ g}\cdot\text{m}^{-2}$ of N and $0.03\text{-}0.06 \text{ g}\cdot\text{m}^{-2}$ of P, G.
232 Gauthier, unpublished data), but was lower than many other Arctic fertilization
233 experiments (*e.g.*, Shaver & Chapin 1995; Gough and Hobbie, 2003; Ylänne *et al.*, 2020).
234 The complete fertilization protocol, applied each year, is available in Pouliot *et al.* (2009).

235 **Field sampling**

236 Field sampling took place during the summer months (primarily July-August) of 2017,
237 2018 and 2019. Fences were deployed over the usually unprotected part of the plot during
238 the sampling year to avoid grazing between the emergence of the vegetation and sampling.
239 Therefore, we measured the long-term impact of fertilization and grazing on ecosystem
240 properties, without capturing the signal of annual disturbance due to goose presence.
241 Temporary fences were removed after sampling to allow late-summer grazing and early
242 season grubbing to resume normally.

243 *Vegetation*

244 We harvested vascular plants and mosses in grazed and ungrazed subplots at the peak of
245 the 2018 growing season (between July 25, 2018 and August 3, 2018). Using a knife, we
246 extracted four 10 cm x 10 cm x 10 cm clods randomly chosen in an 80 cm x 80 cm grid
247 covering half of each subplot. We counted the number of vascular ramets of each species
248 in each clod and summed them to obtain total vascular plant density per subplot in $\text{ind}\cdot\text{m}^{-2}$.
249 Vascular plant biomass ($\text{g}\cdot\text{m}^{-2}$) was obtained by weighing green parts of plants sampled
250 in a subplot after drying them 48 h in a furnace at 60° C. In each clod, a 19.6 cm^2 circular
251 subsample was harvested using a cylinder with cutting edges to sample mosses through the
252 10 cm depth of the clod. Bryophytes of three out of four subsamples were sorted at the
253 species level and weighed after drying to obtain green biomass per species. Again, species
254 biomasses were summed to obtain a total green moss biomass per subplot, in $\text{g}\cdot\text{m}^{-2}$. We
255 limited vegetation sampling within one half of the subplots, to let an undisturbed area for
256 the 2019 measurements. All the subplots in a block were harvested the same day and treated
257 in the two following days.

258 Leaf area index (LAI) and dead vascular plant biomass were measured in 2018 and 2019,
259 respectively. LAI was estimated per subplot using the mean leaf area of each species, their
260 density in the plot and their mean number of leaves (Appendix A). For dead vascular plant
261 biomass, two or three 10 cm x 10 cm x 10 cm clods were selected arbitrarily in every
262 subplot to represent standing vegetation. Standing dead parts of plant individuals and dead
263 parts on the ground were separated from green parts and weighted dry to obtain a dead
264 biomass for each subplot, in g·cm².

265 *Thaw depth and soil volumetric water content*

266 Thaw depth and soil water content were measured repeatedly during the 2017, 2018 and
267 2019 summer. Thaw depth was measured physically using a graduated steel probe driven
268 into the soil down to the frozen part. Because of different sampling period length allowed
269 in the field, we measured thaw depth two times in 2017, four times in 2018 and six times
270 in 2019, from early June to mid-August. At each visit, we measured thaw depth at two to
271 four locations in each subplot depending upon the year. Soil volumetric water content
272 (SWC) was measured one, three and four times in 2017, 2018 and 2019, respectively. In
273 2017 and 2018, we measured SWC at three and four locations per subplot using a WET-2
274 WET sensor coupled to a HH2 moisture meter (Delta T Devices Ltd), respectively. In 2019,
275 SWC was measured at a unique location, using an Hydraprobe (Stevens). To ensure
276 compatibility of the results, we used raw permittivity (ϵ) of both machine and converted it
277 back to SWC using default HH2 calibration such as $SWC = \sqrt{(\sqrt{\epsilon} - 1.6)/8.4}$. Each subplot
278 within a block was measured within 2 h on the same day, and measurements taken in a
279 subplot were averaged to give a value per subplot per date.

280 *Distance between surface and water table*

281 Distance between soil surface and water table was measured four times in each subplot
282 during the 2019 growing season. About 8.25 cm diameter and 1 m deep holes were drilled
283 in each plot early in June 2019. At each subplot visit, the distance was measured in cm
284 using a graduated probe. If there was no liquid water, the distance between surface and ice
285 was used.

286 *Albedo*

287 We measured repeatedly incident and reflected radiations during the 2018 (three times) and
288 2019 (four times) summers using a radiometer (SKR 1850/S light sensor, coupled to a
289 SpectroSense2+ logger, Skye). Measurements were made around four wavelengths: blue
290 (466±19 nm), green (556±22 nm), red (644±51 nm) and Near Infra-Red (NIR, 860±37 nm).
291 Incident radiations were captured with a cosine-corrected sensor. Sensors were placed on
292 a handheld pole keeping the reflected light sensor 150 cm above the soil surface,
293 representing a 0.35m² surface of measurement for reflected radiation. We measured
294 radiations at four (2018) or two (2019) different locations within each subplot and averaged
295 them per subplot per date. Horizontality of sensors was checked with a level. We calibrated
296 reflectance (the ratio between incident and reflected radiations) per band against six
297 Spectralon® standards of known reflectance (2%, 5%, 10%, 20%, 40% and 50%
298 reflectance). We then computed albedo using the *albedo* function in the *microclima* R
299 package (Maclean *et al.*, 2019), weighting corrected reflectance of each band by its relative
300 energy contribution along all the measured bands. Each treatment of a block was measured
301 during a 1 h interval.

302 *Soil physical properties*

303 Soil cores (10 cm x 10 cm) were harvested in each subplot at the beginning of August 2019
304 (except for one lost sample in one grazed control). Soil was sampled down to
305 approximately 20 cm. After bringing refrigerated samples to the University of Quebec at
306 Trois-Rivières, thermal conductivity was measured at 5, 10 and 15 cm (when possible)
307 using a TP08 non-steady-state probe (Hukseflux), inserted into a copper made insertion
308 guide, coupled to a Campbell CR1000 datalogger (Appendix B). Valid measurements (as
309 defined in appendix B) were averaged to obtain a mean value per sample per depth.

310 After thermal conductivity measurements, soil samples were photographed and separated
311 by visually homogeneous horizons. For each horizon, we determined the organic matter
312 content as the Loss-On-Ignition (LOI, $\text{g}\cdot\text{g}^{-1}$), calculated using the dry weight (W_d) and the
313 burned weight (W_b) as $(W_d - W_b)/W_d$. Soil LOI is linearly related to soil C content in highly
314 organic peat (Bhatti & Bauer, 2002; Klingenfuß *et al.*, 2014). We then computed dry
315 density and porosity using the equations and the compiled values in Balland and Arp (2005,
316 details in appendix B). These three variables link the biological processes driving SOM
317 accumulation to the thermal conductivity of soil. For example, we expect less decomposed
318 SOM to form a soil less dense and more porous, than in case of more decomposed SOM.
319 This high soil porosity could lead to low conductivity if pores are filled with air, or to high
320 conductivity if pores are filled with water.

321 **Data analysis**

322 *Statistical analysis*

323 We used linear mixed effect models and generalized additive mixed models (GAMMs) to
324 estimate interactive effects of fertilization and grazing. Each model contained discrete
325 fertilization treatments (with levels Control, Low N, High P, High N, High N+P), grazing
326 status and the interaction between fertilization and grazing as fixed effects. Details of
327 models' structure and transformation are presented in Table 1.

328 Following Amrhein *et al.* (2019), we avoided discrete thinking by not choosing a *p-value*
329 threshold guiding statistical inference. Instead, we highlighted a statistically supported
330 effect by analysing both the *p-value* of the factor continuously and considering the
331 magnitude and 95 % confidence interval of the post-hoc differences between the control
332 and other experimental treatments.

333 All statistical analyses were calculated with R 4.0.3 (R Core Team, 2020). Mixed effects
334 models were fitted using the *lme4* package (Bates *et al.*, 2014) and inferences were made
335 using functions in *lmerTest* (Kuznetsova *et al.*, 2017). GAMMs were fitted using the *gam*
336 function and in the *mgcv* package (Wood, 2011), random effects being represented as
337 penalized regression terms. Treatment marginal means and inferences about contrasts were
338 estimated using the *emmeans* package (Lenth, 2021).

339

340 Table 1 : Description of data, model structure and transformation (Transf.) for each variable analysed in this
 341 study. Transformations were selected to ensure normality of residuals. Each model contained fertilization (F,
 342 five levels), grazing (G) status and their interaction as fixed effects. Random effects structure was determined
 343 following Gumpertz and Brownie (1992).

Variable	Transf.	Measurements	Fixed effects	Random effects
Vascular plant biomass	<i>none</i>	Unique value per subplot (2018)	Block	Plot
Leaf area index	<i>logit</i>	$n = 40$		
Bryophyte biomass	<i>log</i>			
Dead vascular plant biomass	<i>log</i>			
Soil Loss-on-Ignition	<i>logit</i>	Unique value for each horizon of each subplot, weighted by the relative thickness of the horizon (2019)	Block	Plot
Soil dry density	<i>log</i>			Subplot
Soil porosity	<i>logit</i>	$n = 39 \times \text{number of horizons in each soil column}$		Third order cubic spline along depth for each F x G level (GAMM)
Soil thermal conductivity	<i>log</i>	Mean value at 5 and 10 cm depth for each subplot (2019) $n = 39 \times 2 \text{ depths}$	Block Depth (two levels) Depth x Fertilization Depth x Grazing Depth x F x G	Plot Subplot
Water table depth	<i>none</i>	Mean value per subplot (2019) $n = 40$	Block	Plot
Albedo	<i>logit</i>	Mean value per subplot per year (2017, 2018, 2019)	Block	Plot
Soil Volumetric Water Content	<i>none</i>		Year	Subplot
Thaw depth	<i>none</i>	$n = 40 \times 3 \text{ years}$	Year x Block Year x Fertilization Year x Grazing Year x F x G	Year x Plot

344

345 *Numerical modelling*

346 We used a numerical heat transfer model with phase change to disentangle the effect of
 347 changes in surface and soil properties on active layer thaw. Using marginal means of soil
 348 parameters of the grazed and ungrazed Control and High N+P treatments, we examined
 349 what part of the observed variation in thaw depth may be attributed to change in soil
 350 properties. We explored two scenarios: the “Soil scenario” reproduced the differences
 351 among treatments in term of soil properties only, with fixed albedo. The “Soil+Albedo

352 scenario” implemented the observed differences in both soil properties and albedo.
353 Developing a complete radiative and land-surface modelling was beyond the scope of the
354 study, so we evaluated the impact of surface properties by interpreting the difference
355 between observed and modelled thaw depth. Preliminary results showed that thaw depth
356 was insensitive to variation in snow depth or depth hoar formation during the five year of
357 the modelling experiment, max snow depth ranging from 0.10 to 0.36 m. We thus used the
358 observed snow depth with similar snow properties for all scenario and treatments.
359 Complete model specification is available in Appendix C and Chen *et al.* (2021).

360 **Results**

361 Fertilization increased vascular plant biomass, but grazing had no effect (Table 2, Fig. S1),
362 whereas neither fertilization nor grazing impacted bryophyte biomass (Table 2, Fig. S2).
363 Vascular plant biomass of High N+P plots was 318% higher than biomass of Control plots
364 [mean effect (95% confidence interval, ci): 69.8 (45.0;94.6) g·m⁻²].

365 *Surface properties*

366 Fertilization increased green Leaf Area Index (LAI), but grazing had no effect (Fig. 1b,
367 Table 2), whereas grazing reduced dead vascular plant biomass with little effect of
368 fertilization (Fig. 1c, Table 2). LAI of High N+P plots was 345% higher than LAI of Control
369 plots [mean effect (95% ci): 0.54 (0.34;0.73) m²·m⁻²]. Grazed subplots had a dead vascular
370 plant biomass 60.0% lower than ungrazed subplots [mean effect (95% ci): -15.6 (-7.69;-
371 23.4) g·m⁻²].

372 Fertilization increased surface albedo whereas grazing decreased it (Fig. 1a, Table 3). For
373 example, albedo of High N+P plots was higher by 79% [mean effect (95% ci): 0.05
374 (0.03;0.08)] than albedo of Control plots. Grazed subplots had a 25% lower albedo [mean
375 effect (95% ci): 0.03 (0.02;0.03)] than ungrazed ones. Grazing effect was slightly reduced
376 in more fertilized plots. For example, grazed Control had a 32% lower albedo than the
377 respective ungrazed subplots [mean effect (95% ci): -0.03 (-0.02;-0.04)] whereas ungrazed
378 High N+P had a 10.8% lower albedo than High N+P ungrazed subplots [mean effect (95%
379 ci): -0.02 (-0.03;0.01)].

380 **Table 2:** Results of the linear mixed models and generalized additive mixed models fitted to estimate the
381 impact of fertilization (F) and goose grazing (G) on Leaf Area Index (LAI); dead vascular plant biomass;

382 bryophyte biomass; soil Loss-on-Ignition, dry bulk density and porosity; distance between soil surface and
 383 water table and soil thermal conductivity in wetlands of Bylot Island, Nunavut, Canada.

	Fertilization			Grazing			Block			FxG		
	<i>df</i>	<i>F</i>	<i>P</i>	<i>df</i>	<i>F</i>	<i>P</i>	<i>df</i>	<i>F</i>	<i>P</i>	<i>df</i>	<i>F</i>	<i>P</i>
Vascular biomass	4,23	30.2	<0.001	1,23	0.273	0.606	3,23	7.12	0.002	4,23	1.25	0.317
Bryophyte biomass	4,10	1.15	0.388	1,13	0.03	0.858	3,10	8.35	0.005	4,13	2.82	0.069
Leaf Area Index	4,10	12.7	0.001	1,13	0.01	0.912	3,10	1.47	0.230	4,13	1.7	0.268
Dead vascular biomass	4,12	3.17	0.054	1,15	29.0	<0.001	3,12	2.63	0.098	4,15	0.97	0.455
Soil Loss-On-Ignition	4,145	10.2	<0.001	1,145	1.05	0.307	3,145	70.4	<0.001	4,145	2.49	0.046
Soil dry density	4,139	6.66	<0.001	1,139	1.62	0.206	3,139	24.8	<0.001	4,139	1.82	0.128
Soil Porosity	4,137	5.16	0.001	1,137	1.41	0.238	3,137	18.2	<0.001	4,137	1.5	0.218
Distance to water table	4,27	10.7	<0.001	1,27	11.9	0.002	3,27	7.84	0.001	4,27	0.40	0.810
Soil thermal conductivity	4,24	2.88	0.044	1,24	11.7	0.002	3,24	1.42	0.262	4,24	1.00	0.432

384

385

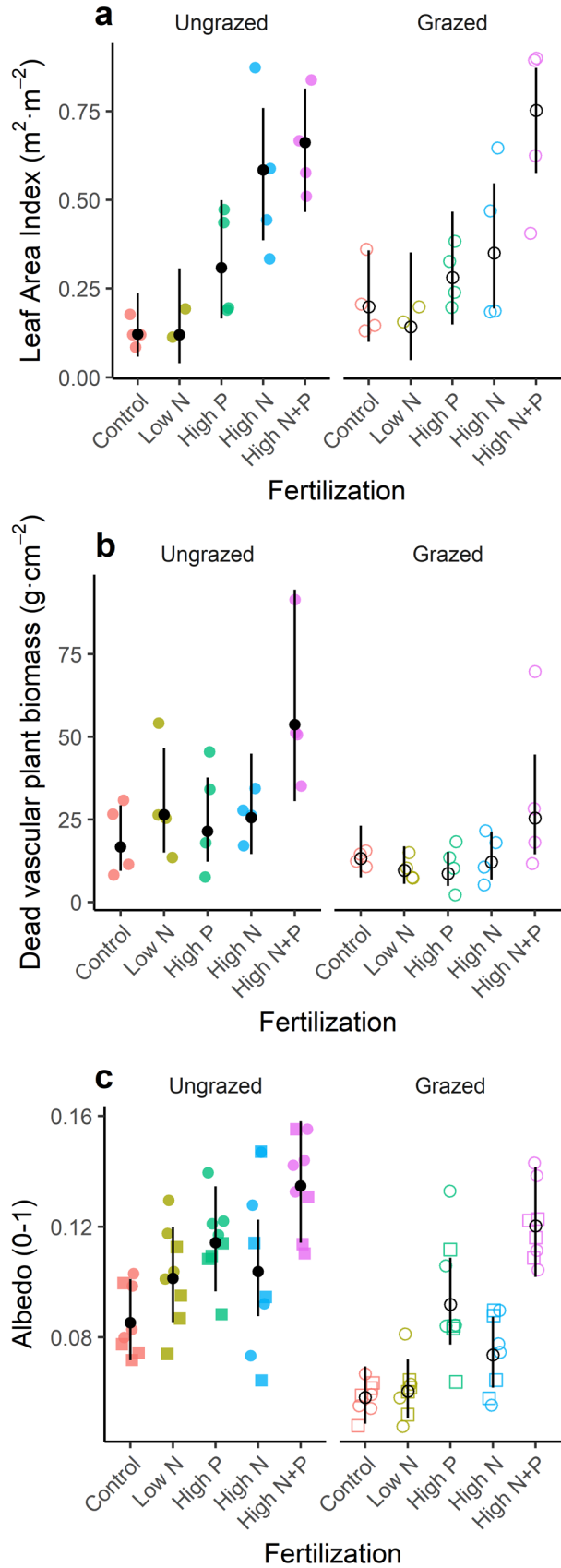


Figure 1: Effect of fertilization treatments and goose grazing on a) albedo, b) green leaf area index (LAI) and c) dead vascular plant biomass in wetlands of Bylot Island, Nunavut, Canada. Colored points are measured values. Plain and open symbols represent ungrazed and grazed treatments, respectively. Colored circles and squares represent measurements made in 2018 and 2019, respectively. Black points represent each treatment marginal mean, and the line the 95% confidence interval.

400 **Table 3:** Results of the linear mixed models fitted to estimate the impact of fertilization and grazing on
 401 albedo; topsoil volumetric water content (0-5cm depth, SWC) and thaw depth in wetlands of Bylot Island,
 402 Nunavut, Canada.

	Albedo			SWC			Thaw depth		
	<i>df</i>	<i>F</i>	<i>P</i>	<i>df</i>	<i>F</i>	<i>P</i>	<i>df</i>	<i>F</i>	<i>P</i>
Fertilization	4,12	10.7	0.001	4,11	4.91	0.015	4,12	1.87	0.180
Grazing	1,14	79.4	<0.001	1,15	22.9	0.001	1,15	9.70	0.007
FxG	4,14	3.65	0.029	4,15	2.06	0.138	4,15	0.65	0.633
Block	3,12	0.81	0.510	3,11	0.93	0.456	3,12	1.12	0.380
Year	1,12	12.8	0.004	2,24	15.2	<0.001	2,23	35.8	<0.001
YxB	3,12	0.87	0.482	6,24	2.09	0.092	6,23	1.47	0.233
YxF	4,12	0.90	0.496	8,24	0.61	0.765	8,23	0.75	0.648
YxG	1,15	2.87	0.111	2,30	1.72	0.197	2,29	0.66	0.524
YxFxG	4,15	0.31	0.865	8,30	0.49	0.852	8,29	0.47	0.868

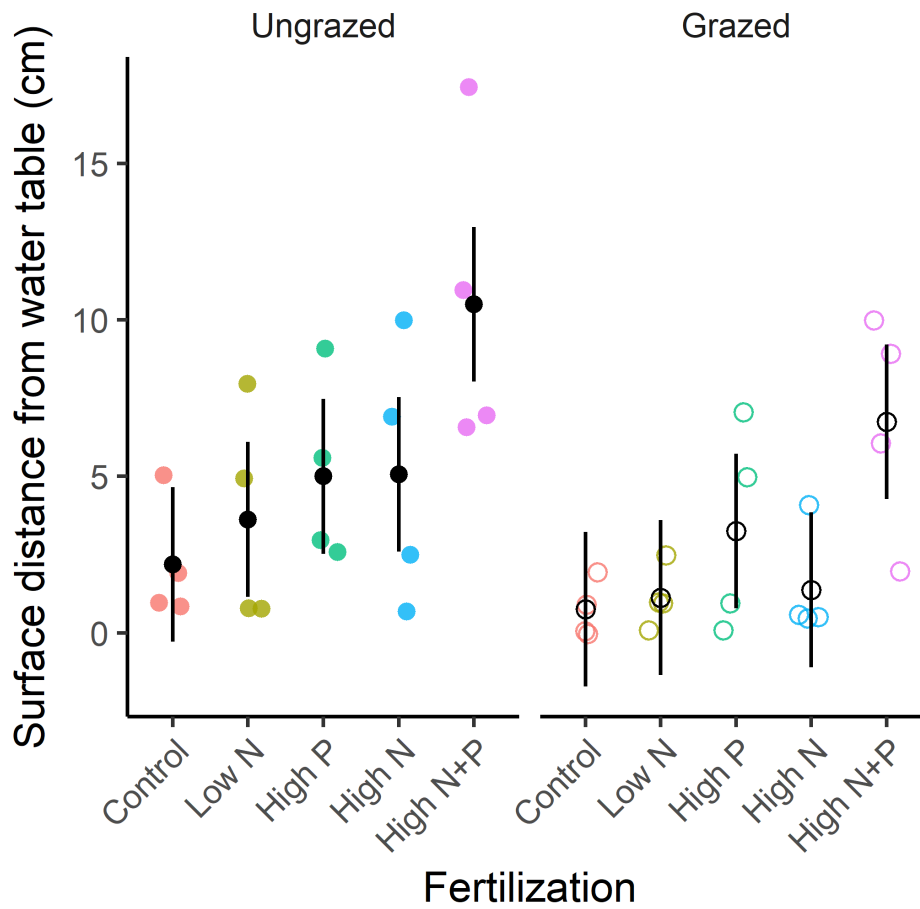
403

404

405 *Soil organic matter accumulation and properties*

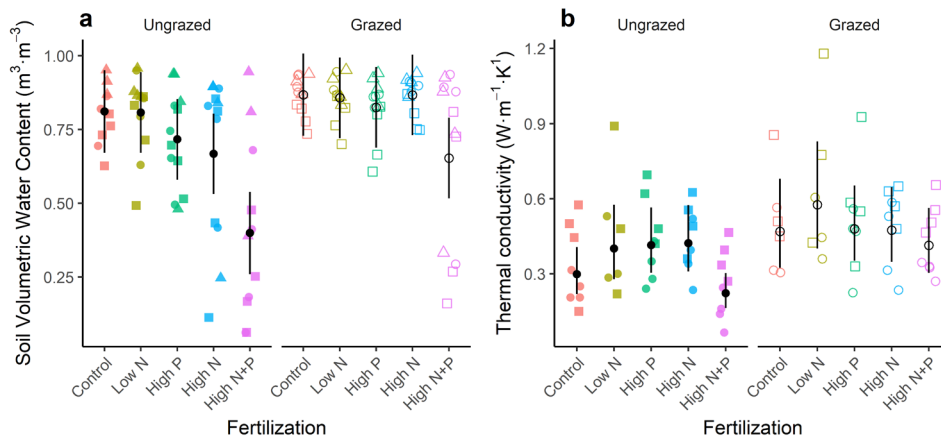
406 By adding new barely decomposed organic horizons at the top of the soil column (Fig. S3,
 407 S4), fertilization increased the distance between the surface and the water table, whereas
 408 grazing decreased it (Fig. 2, Table 2). For example, the land surface was 486% further from
 409 the water table in High N+P plots than in Control plots [mean effect (95% ci): 7.16
 410 (3.99;10.3) cm]. On average, the surface of grazed subplots was 50% closer to the water
 411 table than the surface of ungrazed ones [mean effect (95% ci): -2.62 (-1.05;-4.2) cm].

412 Fertilization favored dry topsoil conditions (Fig. 3a, Table 3, topsoil referring
 413 approximately to the shallowest 5 cm of the soil column), creating soil characterized by
 414 low dry bulk density, high LOI and high porosity (Table 3, Fig. S4-6) whereas grazing
 415 maintained the soil wetter (Fig. 3a, Table 3). For example, SWC was 37% lower in the
 416 High N+P plots than in the Control [mean effect (95% ci): -0.31 (-0.52;-0.1) m³·m⁻³],
 417 whereas it was 20% higher in grazed subplots than in ungrazed ones [mean effect (95% ci):
 418 0.1 (0.07;0.19) m³·m⁻³].



419

420 **Figure 2:** Effect of fertilization and grazing treatments on distance between soil surface and the water table
 421 in wetlands of Bylot Island, Nunavut, Canada. Colored points are measured values. Plain and open symbols
 422 represent ungrazed and grazed treatments, respectively. Black points represent each treatment marginal mean,
 423 and the line the 95% confidence interval.

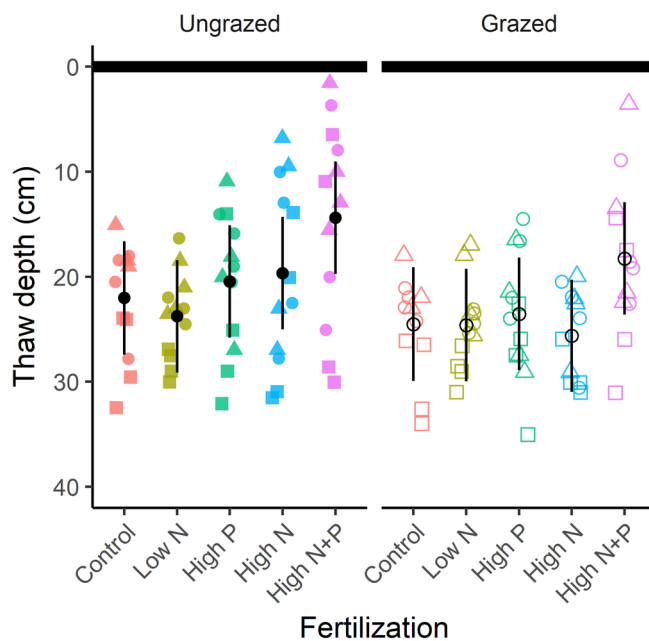


424

425 **Figure 3:** Effect of fertilization and grazing treatments on a) topsoil volumetric water content and b) soil
 426 thermal conductivity in wetlands of Bylot Island, Nunavut, Canada. Colored points are measured values. In
 427 panel a), colored triangles, circles and squares represent measurements made in 2017, 2018 and 2019,

428 respectively. In panel b), colored circles and squares represent measurements made at 5 and 10 cm depth,
 429 respectively. Black points represent each treatment marginal mean, and the line the 95% confidence interval.

430 Grazing increased thermal conductivity (Table 2, Fig. 3b), whereas the fertilization effect
 431 was weak and too uncertain to be interpreted [e.g., High N+P – Control = -0.05 (-0.22;0.11)
 432 $\text{W}\cdot\text{m}^{-1}\cdot\text{K}^{-1}$, mean (95% ci)]. Grazed subplots had a thermal conductivity 38% higher than
 433 ungrazed ones [mean effect (95% ci): 0.131 (0.03;0.22) $\text{W}\cdot\text{m}^{-1}\cdot\text{K}^{-1}$]. Thermal conductivity
 434 increased with depth (p -value < 0.001, Fig. S7). The higher thermal conductivity in grazed
 435 treatment was caused by the higher SWC in these subplots. Adding SWC as a covariate in
 436 the linear mixed model predicting thermal conductivity canceled the effect of grazing
 437 (Fertilization: p -value = 0.510; Grazing: p -value = 0.730, Fig. S8). Computed frozen
 438 thermal conductivity showed a similar pattern, with soil of High N+P being less conductive
 439 than soil of Control plots and the soil of grazed subplots being more conductive than the
 440 soil of ungrazed subplots (Appendix C, table C6).



441

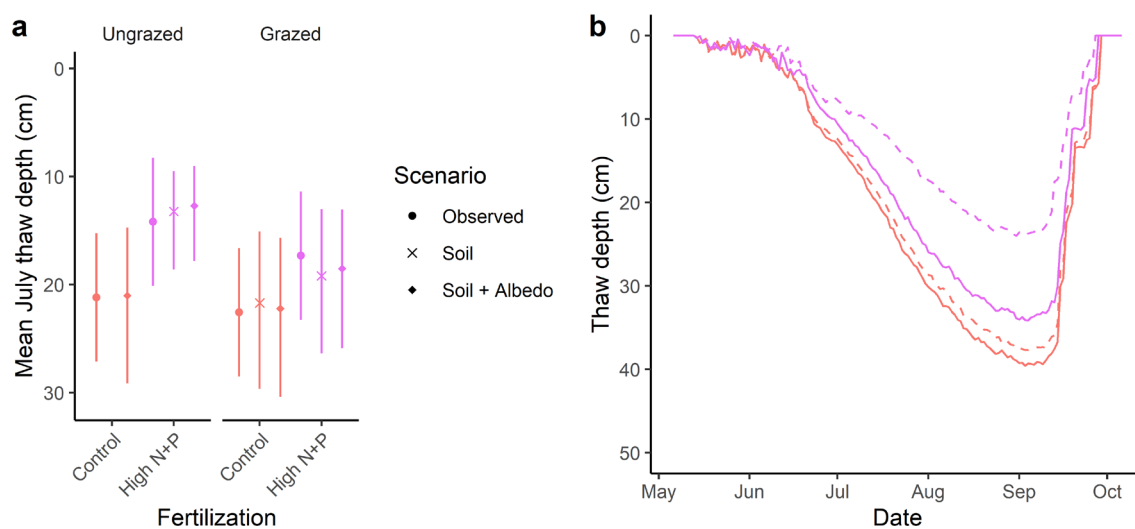
442 **Figure 4:** Effect of fertilization and grazing treatments on thaw depth. Colored points are measured values
 443 in wetlands of Bylot Island, Nunavut, Canada. Black horizontal line represents soil surface. Plain and open
 444 symbols represent ungrazed and grazed treatments, respectively. Colored triangles, circles and squares

445 represent measurements made in 2017, 2018 and 2019, respectively. Black points represent each treatment
446 marginal mean, and the line the 95% confidence interval. Note the inverted y-axis, zero representing soil
447 surface.

448 *Thaw depth*

449 Grazing increased thaw depth, with strong variations of average thaw depth among years
450 (Tab. 3, Fig. 4). Grazed subplots had a 16% lower thaw depth than ungrazed ones [mean
451 effect (95% ci): 3.25 (1.10;5.40) cm].

452 Modelling of thaw depth dynamics supported the effect of grazing on thaw depth (Fig. 5),
453 mainly driven by an increase of topsoil thermal conductivity (“Soil” scenario in Fig. 5a).
454 Increasing albedo from 0.06 (grazed Control) to 0.14 (ungrazed High N+P) had a negligible
455 effect on thaw depth (“Soil + Albedo” scenario in Fig. 5a). Modelling results suggested an
456 interaction between fertilization and grazing, grazing effect being greater in the High N+P
457 treatment than in the Control (Fig. 5a, b). Maximum difference among treatments arose at
458 the end of the thawing season (beginning of September), suggesting that empirical results
459 based on measured July thaw depth are conservative (Fig. 5b).



460

461 **Figure 5:** Modelled effect of fertilization and grazing on thaw depth. a) observed and modeled mean July
462 thaw depth in 2018, and b) modelled dynamic of thaw depth along the thawing season in the “Soil + Albedo”
463 scenario, averaged over all the modelling years. Only differences in soil properties among treatments were

464 implemented in the “Soil scenario”, whereas the “Soil + Albedo” scenario implemented both differences in
465 soil properties and albedo. “Soil” scenario is absent from the ungrazed Control, as it represents the reference
466 from which parameters are modified. Red and purple colors represent Control and High N+P treatments,
467 respectively. Plain and dashed lines represent grazed and ungrazed situations, respectively. Note the reversed
468 *y-axis*.

469 **Discussion**

470 Our results reveal that both N and P availability and grazing impact active layer and
471 permafrost dynamics in High Arctic polygonal wetlands. Fertilization increased live
472 vascular plant cover and albedo, decreasing the radiative energy entering the plant-soil
473 system. Therefore, enhanced herbaceous tundra growth following higher nutrient
474 availability may attenuate the increase of surface temperature due to global warming.
475 Fertilization also increased SOM accumulation at the top of the soil column, changing soil
476 physical structure and composition and increasing permafrost aggradation rate. This
477 suggests that increased topsoil nutrient availability speeds up upward permafrost
478 development rate. Goose grazing reduced albedo and dead vascular plant biomass,
479 increasing the energy entering the plant-soil system. In addition, grazing reduced SOM
480 accumulation and soil thermal conductivity, deepening the active layer. These last results
481 point toward a novel and important perspective, which suggests that grazers may limit
482 syngenetic permafrost development.

483 The decrease in thaw depth and SWC accelerated the transition from *Cyperaceae* to grasses
484 following increased topsoil nutrient availability whereas grazing slowed down such
485 changes and maintained species preferred by geese. Increased topsoil nutrient availability
486 may limit the availability of nutrient at depth by limiting thaw depth. Therefore, reduction
487 of thaw depth may cause a negative feedback disadvantaging the growth of deep-rooting
488 plants, such as plants from the *Cyperaceae* family (Wang *et al.*, 2017). Favored *Poaceae*

489 growth (Wang *et al.*, 2017), soil drying, and shallower thaw depth may all concur to the
490 competitive exclusion of sedges (*Carex aquatilis*) and cotton grasses (*Eriophorum spp.*) in
491 case of increased subsurface nutrient availability (as shown by Gignac *et al.*, 2022 and
492 Nishizawa *et al.*, 2021 in the present experiment). Conversely, goose grazing increases
493 topsoil water content and deepens thaw depth. Thus, grazing indirectly favor the growth of
494 plants preferred by geese, such as *Eriophorum scheuzeri* (as shown by Nishizawa *et al.*,
495 2021 in the present experiment). This suggests that geese can concur to maintain polygonal
496 wetlands in a state favorable for their feeding, despite marked increase in nutrient
497 availability.

498 *Surface properties*

499 As expected in H1, fertilization increased live LAI due to an increase in primary production
500 (the impact of fertilization on live biomass is discussed in Gignac *et al.*, 2022), whereas
501 grazing diminished dead biomass, probably decreasing and increasing the quantity of
502 shortwave radiations reaching the soil surface, respectively. Similar to our results, Prager
503 *et al.* (2017) found that fertilization increased LAI in a moist acidic tundra. Grazing did not
504 impact vascular plant biomass nor LAI. Because grazed subplots were protected during the
505 sampling year, we measured undisturbed growth from the below-ground parts. Therefore,
506 vascular plant communities seem to be resilient to long-term grazing, which is coherent
507 with the demonstrated regrowth ability of dominant grasses (Mattheis & Tieszen 1976, Bakker
508 & Loonen 1998) and sedges (Archer & Tieszen 1983, Raillard & Svodoba 1999) in Arctic wetlands
509 (Beaulieu *et al.*, 1996).

510 A sensitivity analysis considering multiple parameters of tundra surface energy budget
511 (Beringer *et al.*, 2002) showed LAI having a non-linear impact on ground heat flux, with

512 greatest reduction when LAI was around one. Measured live LAI was lower than one, but
513 total cover including dead biomass should reach this threshold. Similarly, Juszak *et al.*
514 (2016, 2017) described sedge dominated tundra with a total LAI of 1.4, dead vascular
515 leaves representing half of the total leaf area. Therefore, both live and dead leaf area index
516 influence tundra radiation budget. Overall, our results suggest that nutrient availability may
517 decrease and grazing increase transmission of radiation to the ground in herbaceous tundra.

518 As expected in H1, fertilization increased surface albedo, whereas grazing decreased it.
519 Higher albedo resulted from greater LAI (Juszak *et al.*, 2014) and light-colored litter cover
520 (Juszak *et al.*, 2017), but also possibly from the lower moss water content in the more
521 fertilized plots (Kim & Verma, 1996). The switch from dark mosses (*Drepanocladus spp.*
522 being dominant in Control plots) to light green mosses (*Aulacomnium spp.* being dominant
523 in N+P plots, Gignac *et al.*, 2022) may also have contributed to increase albedo.
524 Conversely, grazing reduced albedo mostly by increasing topsoil water content and
525 reducing light-colored dead vascular plant biomass accumulation. Our results clearly show
526 N and P availability and grazing respectively increase and decrease summer albedo in a
527 High Arctic system even without deciduous shrubs, which had not yet invaded our
528 experimental plots after 16 years. However, surface albedo may not be the most
529 determinant parameter for ground heat flux and active layer thaw, as higher transmission
530 of shortwave radiations through the canopy to the ground may counteract an increase in
531 albedo (Blok *et al.*, 2010). Modelling experiment suggested a negligible effect of albedo
532 on thaw depth.

533 Even if our results suggested diminished shortwave radiation input to the ground in
534 response to fertilization, the consequences for net radiation budget and ground heat flux

535 are hard to estimate. Cooler vegetation and soil surface may emit less longwave radiations
536 than warmer vegetation and soil, leading to similar budget even with differences in net
537 shortwave input (Juszek *et al.*, 2016).

538 The observed change in vegetation and SWC may have impacted heat flux partitioning.
539 Eugster *et al.* (2005) reported that tundra with lower LAI has a smoother surface (lower
540 roughness length) than tundra with higher LAI, but it did not impact latent and sensible
541 heat fluxes. Increased LAI may increase latent heat flux (McFadden *et al.*, 1998), but
542 surface drying following fertilization and protection from grazing likely resulted in lower
543 evaporation (Liljedhal *et al.*, 2011). It is however uncertain whether a change in surface
544 resistance at this scale would impact the soil heat flux, or if latent and sensible heat fluxes
545 would change at the expense of one another (McFadden *et al.*, 1998).

546 *Organic matter accumulation*

547 As expected in H2, fertilization increased SOM accumulation at the top of the soil column,
548 whereas grazing decreased it. SOM accumulation followed a substantial increase in
549 vascular plant primary productivity in fertilized treatments, especially when N and P were
550 added together (Gignac *et al.*, 2022). Topsoil SOM accumulation after long-term
551 fertilization has been measured by Mack *et al.* (2004) in a moist acidic Arctic tundra, but
552 the effect is not general (see *e.g.*, Koyama *et al.*, 2013 and Yläne *et al.* 2020). The impact
553 of goose grazing and grubbing on soil OM is not clear either, with both negative (*e.g.*,
554 Sjögersten *et al.*, 2012; van der Wal *et al.*, 2007) and null effects (*e.g.*, Speed *et al.*, 2010)
555 being reported in similar systems.

556 Because fertilization increased surface aggradation without impacting thaw depth, it
557 implies permafrost table shall have migrated upward at a greater rate in fertilized plots than
558 in control ones. Considering the historical aggradation rate of $0.7 \text{ mm}\cdot\text{year}^{-1}$ measured at
559 our study site (Fortier *et al.*, 2006), the surface of Control plots should have risen by
560 approximately 11 mm in 16 years. Assuming that the water table is homogeneous in a
561 polygon, we consider that a higher distance between the soil surface and the water table
562 implies higher surface aggradation. Therefore, the surface of High N+P plots had on
563 average risen 72 mm above the surface of Control plots (Fig. S9). Fertilization had thus
564 multiplied the aggradation rate by up to seven times relative to the historical rate (5
565 $\text{mm}\cdot\text{year}^{-1}$ in the High N+P plots). However, grazing slowed down surface aggradation,
566 grazed subplots being on average 26 mm closer to the water table than ungrazed ones.
567 Therefore, grazing limited the uplifting related to fertilization, surface of grazed High N+P
568 plots having risen by approximately 57 mm only during the 16 years of the experiment (for
569 an aggradation rate of $3.6 \text{ mm}\cdot\text{year}^{-1}$). These results point toward an important role of
570 grazers in limiting both polygon development and permafrost carbon storage in productive
571 polygonal tundra, especially in presence of increased nutrient availability.

572 *Soil thermal properties*

573 SOM accumulation and disconnection from the water table decreased topsoil thermal
574 conductivity. SWC is known to be an important factor controlling thermal conductivity in
575 Arctic soils (Hinzman *et al.*, 1991), a wetter organic soil often leading to higher ground
576 heat flux and deeper thaw depth (see *e.g.*, Liljedahl *et al.*, 2011, Juszak *et al.*, 2016).
577 However, Eugster *et al.* (2005) noted a covariation between heat capacity and thermal
578 conductivity in moist acidic and non-acidic Arctic tundra, high soil temperature being

579 associated with low soil heat flux. Similarly, McFadden *et al.* (1998) noted that the energy
580 stored in soil water was released at night, countering higher midday soil thermal
581 conductivity in wet Arctic tundra.

582 Our results suggested SOM content and porosity alone had little impact on thermal
583 conductivity. SOM content has been recognized as an important driver of thermal
584 diffusivity and active layer thickness across the Arctic (Zhu *et al.*, 2019). Because the
585 present experiment took place at the top of an accumulation of approximately three meters
586 of a mix of peat and loess (Fortier *et al.* 2006) with already high OM content and high
587 porosity ($0.20 \text{ g}\cdot\text{g}^{-1}$ and $0.8 \text{ cm}^3\cdot\text{cm}^{-3}$ on average at the bottom of the sampled soil column),
588 fertilization caused little contrast.

589 Transportation may have partly dried samples prior to measurements, causing a decrease
590 in thermal conductivity. Yet, since we would expect the decrease in SWC and thermal
591 conductivity to be greater in wet samples than in already dry soils, the differences in
592 thermal conductivity may have been reduced by transport, implying that our results are
593 conservative. Because thermal conductivity computation based on soil LOI and field SWC
594 measurements led to qualitatively similar conclusions, and because the modeling
595 experiment reproduced observed thaw depth well, we consider our conclusion to be robust
596 to sample disturbance.

597 *Thaw depth*

598 As hypothesized in H3, grazing increased thaw depth, but contrary to our expectation,
599 fertilization did not impact it. The effect of grazing on thaw depth has been little explored
600 in the literature. Grazing by Muskox has been shown to both decrease (Falk *et al.*, 2015)

601 and increase (Mosbacher *et al.*, 2019) thaw depth in Northeastern Greenland, depending
602 upon the year of measurement. The conservative 3.3 cm average difference we observed
603 between grazed and ungrazed subplots is comparable to what has been measured in several
604 fertilization (6 cm on average in Gough *et al.*, 2016; 4 cm on average in Wang *et al.*, 2017)
605 and surface warming experiments (3 cm on average in Natali *et al.*, 2011; higher thaw rate
606 in Leffler *et al.*, 2016; not supported statistically in Hollister *et al.*, 2006 and Voigt *et al.*,
607 2017). Grazing thus restricted permafrost development by limiting surface aggradation and
608 deepening the active layer. Considering the 3.3 cm increase in active layer depth, grazing
609 reduced permafrost aggradation rate to $1.5 \text{ mm}\cdot\text{year}^{-1}$ in grazed High N+P subplots
610 compared to $5 \text{ mm}\cdot\text{year}^{-1}$ without grazing.

611 Modelling results suggested the decrease of thermal conductivity following fertilization
612 made thaw depth shallower, whereas grazing deepened thaw depth by increasing topsoil
613 thermal conductivity. Thaw depth showed little sensitivity to a decrease of incoming
614 radiation following a more reflective vegetation (similar to Juszak *et al.*, 2016). Previous
615 studies showed that topsoil water content tends to increase thaw depth, especially if deep
616 water and ice content remains constant (Kwon *et al.*, 2016; Clayton *et al.*, 2021).
617 Fertilization effect on thaw depth and the interaction between fertilization and grazing was
618 not supported by our statistical analysis. This may be because of low statistical power, and
619 because plot positioning in the polygon was masking the effect of fertilization, thaw depth
620 being lower in plots close to rims and higher in plots in the vicinity of a water body.
621 Fertilization effects inferred from modelling results were robust to such spatial noise
622 because they represent the addition of a dry organic layer at the top of the soil column,
623 maintain deep soil water and ice content constant and assume no lateral energy transfer.

624 Habitat type deserves consideration when prospecting the effect of increased nutrients
625 availability and varying herbivore population on Arctic ecosystems. We are not aware of
626 studies measuring thaw depth in response to these factors in mesic uplands (e.g. tundra
627 heath and shrub tundra), such as the ones surrounding the studied wetland area. This lack
628 in literature may be related with the physical difficulty encountered with thaw depth
629 measurements in rocky soils (Gough *et al.*, 2016). In such mesic uplands, vascular plant
630 biomass also increases following fertilization (e.g., Grellman, 2002; van Wijk *et al.*, 2004).
631 However, it is uncertain if greater primary productivity would lead to aggradation and
632 drying of the surface (Ola *et al.*, 2022). Uplands are often well drained and characterized
633 by epigenetic permafrost, in which case permafrost does not form by the aggradation of the
634 base of the active layer (French, 2017). Finally, uplands are less intensively grazed by geese
635 compared with wetlands (Hughes *et al.*, 2014), with a presumably lower impact of grazing
636 on permafrost dynamic.

637 *Conclusion*

638 We showed in this study that increase of tundra nutrient availability and grazing can create
639 feedback to the active layer dynamic of High Arctic herbaceous tundra. Fertilization caused
640 OM accumulation at the surface, increasing permafrost aggradation rate, suggesting that
641 the growth of vegetation resulting from higher nutrient mineralization may hinder the
642 degradation of permafrost caused by global warming in herbaceous polygonal tundra.
643 Grazing reduced surface aggradation and deepened the active layer, primarily because of
644 increased topsoil water content. Grazers seem therefore to be a major determinant of the
645 future of permafrost in herbaceous polygonal wetlands, especially while nutrient
646 availability increases in this system. Therefore, population management and resource

647 availability in the south, which can cause strong increase in herbivorous populations
648 migrating to the Arctic in summer (Lefebvre *et al.*, 2017), may indirectly slow down
649 permafrost development in the North. However, the net effect of grazing on polygonal
650 wetlands carbon budget remains unclear, as water saturation of the shallowest soil horizons
651 may limit decomposition (Boye *et al.*, 2017) and concurs to SOM accumulation in Arctic
652 peatlands (Grosse *et al.*, 2011). Overall, our results point toward the importance of
653 understanding impact of biotic drivers when examining potential consequences of climate
654 change on the permafrost of High-Arctic wetlands.

655 **Supplementary materials**

656 **Appendix A:** Details on the measurement of leaf area index.

657 **Appendix B:** Details on the measurement of soil physical and thermal properties.

658 **Appendix C:** Detail of the set-up of the modeling experiment.

659 **Fig. S1:** Impact of fertilization and grazing on vascular plant biomass.

660 **Fig. S2:** Impact of fertilization and grazing on bryophytes biomass.

661 **Fig S3:** Pictures of the soil columns of contrasted treatments.

662 **Fig. S4:** Impact of fertilization and grazing on soil Loss-On-Ignition.

663 **Fig. S5:** Impact of fertilization and grazing on soil dry density.

664 **Fig. S6:** Impact of fertilization and grazing on soil porosity.

665 **Fig. S7:** Impact of fertilization, grazing and depth on soil thermal conductivity.

666 **Fig. S8:** Marginal impact of soil volumetric water content, fertilization and grazing on soil
667 thermal conductivity.

668 **Fig S9:** Pictures of plots showing organic accumulation at the surface.

669 **Acknowledgement**

670 We are grateful to the many people who permit the access to the Sirmilik National Park
671 and the long-term ecological monitoring on Bylot Island, including the Mittimatalik
672 community and Parks Canada's staff, with a special thanks to Maryse Mahy. We thank
673 Riika Rinnan and two anonymous reviewers for having contributed to improve the quality

674 and clarity of the paper. This study was supported by the Fonds de Recherche du Québec-
675 Nature et technologies (FRQNT-2018-PR- 208107), the Natural Sciences and Engineering
676 Research Council of Canada (Discovery program), the Network of Centers of Excellence
677 of Canada Arctic Net Northern Scientific Training Program (Polar Knowledge), Université
678 Laval and Université du Québec à Trois-Rivières with the UQTR Chair in Functional
679 Arctic Ecology (2019-2022), the RIVE research center and GRBV research group.
680 Logistical support for fieldwork was provided and organized by the Polar Continental Shelf
681 Program (Natural Resources Canada) and the Centre d'Études Nordiques (CEN) with a
682 special thanks to M.-C. Cadieux and C. Boismenu.

683 **Conflicts of interest**

684 The authors have no conflicts of interest.

685 **Author contributions**

686 **Lucas Deschamps** conceptualized the study; realized field, soil and vascular plant
687 measurements; compiled data; designed and realized statistical analysis; designed
688 modeling experiment; wrote the manuscript.

689 **Vincent Maire** conceptualized and funded the study; organized and realized field
690 sampling; revised the manuscript at all stages.

691 **Lin Chen** designed and realized modeling experiments; revised the final version of the
692 manuscript.

693 **Daniel Fortier** conceptualized the study; revised modeling parameters; revised the final
694 version of the manuscript.

695 **Gilles Gauthier** initiated and maintained the experiment; funded the study; revised the
696 manuscript at multiple stages.

697 **Amélie Morneau** realized field and bryophyte measurements; revised the final version
698 of the manuscript.

699 **Elizabeth Hardy-Lachance** realized field measurements; revised the final version of the
700 manuscript.

701 **Isabelle Dalcher-Gosselin** realized field measurements; revised the final version of the
702 manuscript.

703 **François Tanguay** realized field measurements; revised the final version of the
704 manuscript.

705 **Charles Gignac** realized field and dead biomass measurements; revised the final version
706 of the manuscript.

707 **Jeffrey McKenzie** conceptualized numerical code with Lin Chen; revised the final version
708 of the manuscript.

709 **Line Rochefort** initiated the experiment; funded the study; revised the final version of the
710 manuscript.

711 **Esther Lévesque** maintained the experiment; conceptualized and funded the study;
712 organized field sampling; revised the manuscript at all stages.

713 **Data availability**

714 Data and codes will be available as a Figshare repository at the publication of the
715 manuscript.

716 **References**

- 717 Amrhein, V., Greenland, S., & McShane, B. (2019). Scientists rise up against statistical
718 significance. *Nature*, *567*, 305–307. <https://doi.org/10.1038/d41586-019-00857-9>
- 719 Archer, S., & Tieszen, L. L. (1983). Effects of simulated grazing on foliage and root
720 production and biomass allocation in an arctic tundra sedge (*Eriophorum*
721 *vaginatum*). *Oecologia*, *58*, 92–102. <https://doi.org/10.1007/BF00384547>
- 722 Bakker, C., & Loonen, M. J. J. E. (1998). The Influence of Goose Grazing on the Growth
723 of *Poa arctica* : Overestimation of Overcompensation. *Oikos*, *82*(3), 459–466.
724 <https://doi.org/10.2307/3546367>
- 725 Balland, V., & Arp, P. A. (2005). Modeling soil thermal conductivities over a wide range
726 of conditions. *Journal of Environmental Engineering and Science*, *4*(6), 549–558.
727 <https://doi.org/10.1139/s05-007>
- 728 Bates, D., Mächler, M., Bolker, B., & Walker, S. (2014). Fitting linear mixed-effects
729 models using lme4. *Journal of Statistical Software*, *67*(1), 1–48.
730 <https://doi.org/10.18637/jss.v067.i01>
- 731 Beringer, J., McIlwaine, S., Lynch, A., Chapin, F., & Bonan, G. (2002). The use of a
732 reduced form model to assess the sensitivity of a land surface model to biotic surface
733 parameters. *Climate Dynamics*, *19*(5–6), 455–466. <https://doi.org/10.1007/s00382-002-0237-9>
- 735 Bernes, C., Bråthen, K. A., Forbes, B. C., Speed, J. D. M., & Moen, J. (2015). What are
736 the impacts of reindeer/caribou (*Rangifer tarandus* L.) on arctic and alpine
737 vegetation? A systematic review. *Environmental Evidence*, *4*(1), 1–26.
738 <https://doi.org/10.1186/s13750-014-0030-3>
- 739 Beaulieu, J., Gauthier, G., & Rochefort, L. (1996). The growth response of graminoid
740 plants to goose grazing in a High Arctic environment. *Journal of Ecology*, 905–914.
741 <https://doi.org/10.2307/2960561>
- 742 Bhatti, J. S., & Bauer, I. E. (2002). Comparing loss-on-ignition with dry combustion as a
743 method for determining carbon content in upland and lowland forest ecosystems.
744 *Communications in Soil Science and Plant Analysis*, *33*(15–18), 3419–3430.
745 <https://doi.org/10.1081/CSS-120014535>
- 746 Bliss, L. C., & Matveyeva, N. V. (1992). Circumpolar arctic vegetation. In F. S. Chapin
747 III, R. L. Jefferies, J. F. Reynolds, G. R. Shaver, J. Svoboda, & E. W. Chu (Eds.),
748 *Arctic ecosystems in a changing climate: an ecophysiological perspective* (Vol. 59,
749 p. 89). Academic Press San Diego.

- 750 Blok, D., Heijmans, M. M. P. D., Schaepman-Strub, G., Kononov, A. V., Maximov, T.
751 C., & Berendse, F. (2010). Shrub expansion may reduce summer permafrost thaw in
752 Siberian tundra. *Global Change Biology*, *16*(4), 1296–1305.
753 <https://doi.org/10.1111/j.1365-2486.2009.02110.x>
- 754 Boye, K., Noël, V., Tfaily, M. M., Bone, S. E., Williams, K. H., Bargar, J. R., & Fendorf,
755 S. (2017). Thermodynamically controlled preservation of organic carbon in
756 floodplains. *Nature Geoscience*, *10* (6), 415–419. <https://doi.org/10.1038/ngeo2940>
- 757 Chen, L., Voss, C. I., Fortier D., & McKenzie, J. M. (2021). Surface energy balance of
758 sub-Arctic roads and highways in permafrost regions. *Permafrost and Periglacial*
759 *Processes*, *32*(4): 681-701. <https://doi.org/10.1002/ppp.2129>.
- 760 Clayton, L. K., Schaefer, K., Battaglia, M. J., Bourgeau-Chavez, L., Chen, J., Chen, R.
761 H., ... & Zhao, Y. (2021). Active layer thickness as a function of soil water
762 content. *Environmental Research Letters*, *16*(5), 055028.
- 763 Eugster, W., McFadden, J. P., & Stuart Chapin, F. (2005). Differences in Surface
764 Roughness, Energy, and CO₂ Fluxes in Two Moist Tundra Vegetation Types,
765 Kuparuk Watershed, Alaska, U.S.A. *Arctic, Antarctic, and Alpine Research*, *37*(1),
766 61–67. [https://doi.org/10.1657/1523-0430\(2005\)037\[0061:DISREA\]2.0.CO;2](https://doi.org/10.1657/1523-0430(2005)037[0061:DISREA]2.0.CO;2)
- 767 Falk, J. M., Schmidt, N. M., Christensen, T. R., & Ström, L. (2015). Large herbivore
768 grazing affects the vegetation structure and greenhouse gas balance in a high arctic
769 mire. *Environmental Research Letters*, *10*(4). [https://doi.org/10.1088/1748-](https://doi.org/10.1088/1748-9326/10/4/045001)
770 [9326/10/4/045001](https://doi.org/10.1088/1748-9326/10/4/045001)
- 771 Fortier, D., Allard, M., & Pivot, F. (2006). A late-Holocene record of loess deposition in
772 ice-wedge polygons reflecting wind activity and ground moisture conditions, Bylot
773 Island, eastern Canadian Arctic. *Holocene*, *16* (5), 635–646.
774 <https://doi.org/10.1191/0959683606hl960rp>
- 775 French, H. M. (2017). *The Periglacial Environment*. John Wiley & Sons: Hoboken, NJ,
776 USA. <https://doi.org/10.1002/9781119132820>
- 777 Gauthier, G., Hughes, R. J., Reed, A., Beaulieu, J., & Rochefort, L. (1995). Effect of
778 Grazing by Greater Snow Geese on the Production of Graminoids at an Arctic Site.
779 *Journal of Ecology*, *83*(4), 653–664. <https://doi.org/10.2307/2261633>
- 780 Gauthier, G., Giroux J. F. & Rochefort., L. (2006). The impact of goose grazing on arctic
781 and temperate wetlands. *Acta Zoologica Sinica*, *52*(supplement):108-111.
- 782 Gignac, C., Rochefort, L., Gauthier, G., Lévesque, E., Maire, V., Deschamps, L., Pouliot,
783 R., & Marchand-Roy, M. (2022). N/P Addition Is More Likely Than N Addition
784 Alone to Promote a Transition from Moss-Dominated to Graminoid-Dominated

- 785 Tundra in the High-Arctic. *Atmosphere*, 13(5), 676.
786 <https://doi.org/10.3390/atmos13050676>
- 787 Gornall, J. L., Jónsdóttir, I. S., Woodin, S. J., & Van der Wal, R. (2007). Arctic mosses
788 govern below-ground environment and ecosystem processes. *Oecologia*, 153(4),
789 931–941. <https://doi.org/10.1007/s00442-007-0785-0>
- 790 Gornall, J. L., Woodin, S. J., Jónsdóttir, I. S., & van der Wal, R. (2009). Herbivore
791 impacts to the moss layer determine tundra ecosystem response to grazing and
792 warming. *Oecologia*, 161(4), 747–758. <https://doi.org/10.1007/s00442-009-1427-5>
- 793 Gough, L., & Hobbie, S. E. (2003). Responses of Moist Non-Acidic Arctic Tundra to
794 Altered Environment : Productivity , Biomass , and Species Richness. *Oikos*, 103(1),
795 204–216. <https://doi.org/10.1034/j.1600-0706.2003.12363.x>
- 796 Gough, L., Bettez, N. D., Slavik, K. A., Bowden, W. B., Giblin, A. E., Kling, G. W., ...
797 Shaver, G. R. (2016). Effects of long-term nutrient additions on Arctic tundra,
798 stream, and lake ecosystems: beyond NPP. *Oecologia*, 182(3), 653–665.
799 <https://doi.org/10.1007/s00442-016-3716-0>
- 800 Grellmann, D. (2002). Plant responses to fertilization and exclusion of grazers on an
801 arctic tundra heath. *Oikos*, 98(2), 190–204. [https://doi.org/10.1034/j.1600-](https://doi.org/10.1034/j.1600-0706.2002.980202.x)
802 [0706.2002.980202.x](https://doi.org/10.1034/j.1600-0706.2002.980202.x)
- 803 Grosse, G., Harden, J., Turetsky, M., McGuire, A. D., Camill, P., Tarnocai, C., Frolking,
804 S., Schuur, E. A. G., Jorgenson, T., Marchenko, S., Romanovsky, V., Wickland, K.
805 P., French, N., Waldrop, M., Bourgeau-Chavez, L., & Striegl, R. G. (2011).
806 Vulnerability of high-latitude soil organic carbon in North America to disturbance.
807 *Journal of Geophysical Research: Biogeosciences*, 116 (3).
808 <https://doi.org/10.1029/2010JG001507>
- 809 Gu, Q., & Grogan, P. (2020). Responses of low Arctic tundra plant species to
810 experimental manipulations: Differences between abiotic and biotic factors and
811 between short- and long-term effects. *Arctic, Antarctic, and Alpine Research*, 52 (1),
812 524–540. <https://doi.org/10.1080/15230430.2020.1815360>
- 813 Gumpertz, M. L., & Brownie, C. (1992). Repeated measures in randomized block and
814 split-plot experiments. *Canadian Journal of Forest Research*, 23, 625–639.
815 <https://doi.org/10.1139/x93-083>
- 816 Hartley, A. E., Neill, C., Melillo, J. M., Crabtree, R., & Bowles, F. P. (1999). Plant
817 Performance and Soil Nitrogen Mineralization in Response to Simulated Climate
818 Change in Subarctic Dwarf Shrub Heath. *Oikos*, 86(2), 331.
819 <https://doi.org/10.2307/3546450>

- 820 Hinzman, L. D., Kane, D. L., Gieck, R. E., & Everett, K. R. (1991). Hydrologic and
821 thermal properties of the active layer in the Alaskan Arctic. *Cold Regions Science*
822 *and Technology*, 19(2), 95–110. [https://doi.org/10.1016/0165-232X\(91\)90001-W](https://doi.org/10.1016/0165-232X(91)90001-W)
- 823 Hodkinson, I. D., Webb, N. R., Bale, J. S., & Block, W. (1999). Hydrology, water
824 availability and tundra ecosystem function in a changing climate: The need for a
825 closer integration of ideas? *Global Change Biology*, 5(3), 359–369.
826 <https://doi.org/10.1046/j.1365-2486.1999.00229.x>
- 827 Hollister, R. D., Webber, P. J., Nelson, F. E., & Tweedie, C. E. (2006). Soil thaw and
828 temperature response to air warming varies by plant community: Results from an
829 open-top chamber experiment in northern Alaska. *Arctic, Antarctic, and Alpine*
830 *Research*, 38(2), 206–215. [https://doi.org/10.1657/1523-](https://doi.org/10.1657/1523-0430(2006)38[206:STATRT]2.0.CO;2)
831 [0430\(2006\)38\[206:STATRT\]2.0.CO;2](https://doi.org/10.1657/1523-0430(2006)38[206:STATRT]2.0.CO;2)
- 832 Hughes, R. J., Reed, A., & Gauthier, G. (1994a). Space and Habitat Use by Greater Snow
833 Goose Broods on Bylot Island, Northwest Territories. *The Journal of Wildlife*
834 *Management*, 58(3), 536–545. <https://doi.org/10.2307/3809326>
- 835 Hughes, R. J., Gauthier, G., & Reed, A. (1994b). Summer habitat use and behaviour of
836 Greater Snow Geese *Anser caerulescens*. *Wildfowl*, 45 49–64.
- 837 Jorgenson, M. T., Romanovsky, V., Harden, J., Shur, Y., O'Donnell, J., Schuur, E. A. G.,
838 ... & Marchenko, S. (2010). Resilience and vulnerability of permafrost to climate
839 change. *Canadian Journal of Forest Research*, 40(7), 1219–1236.
840 <https://doi.org/10.1139/X10-060>
- 841 Juszak, I., Erb, A. M., Maximov, T. C., & Schaepman-Strub, G. (2014). Arctic shrub
842 effects on NDVI, summer albedo and soil shading. *Remote Sensing of Environment*,
843 153, 79–89. <https://doi.org/10.1016/j.rse.2014.07.021>
- 844 Juszak, I., Eugster, W., Heijmans, M. M. P. D., & Schaepman-Strub, G. (2016).
845 Contrasting radiation and soil heat fluxes in Arctic shrub and wet sedge tundra.
846 *Biogeosciences*, 13(13), 4049–4064. <https://doi.org/10.5194/bg-13-4049-2016>
- 847 Juszak, I., Iturrate-Garcia, M., Gastellu-Etchegorry, J. P., Schaepman, M. E., Maximov,
848 T. C., & Schaepman-Strub, G. (2017). Drivers of shortwave radiation fluxes in
849 Arctic tundra across scales. *Remote Sensing of Environment*, 193, 86–102.
850 <https://doi.org/10.1016/j.rse.2017.02.017>
- 851 Kim, J., & Verma, S. B. (1996). Surface exchange of water vapour between an open
852 sphagnum fen and the atmosphere. *Boundary-Layer Meteorology*, 79(3), 243–264.
853 <https://doi.org/10.1007/bf00119440>

- 854 Klingenfuß, C., Roßkopf, N., Walter, J., Heller, C., Zeitz, J. (2014). Soil organic matter to
855 soil organic carbon ratios of peatland soil substrates. *Geoderma*, 235–236, 410–417.
856 <https://doi.org/10.1016/j.geoderma.2014.07.010>
- 857 Koven, C. D., Ringeval, B., Friedlingstein, P., Ciais, P., Cadule, P., Khvorostyanov,
858 D., ... Tarnocai, C. (2011). Permafrost carbon-climate feedbacks accelerate global
859 warming. *Proceedings of the National Academy of Sciences*, 108(36), 14769–14774.
860 <https://doi.org/10.1073/pnas.1103910108>
- 861 Koven, C. D., Lawrence, D. M., & Riley, W. J. (2015). Permafrost carbon–climate
862 feedback is sensitive to deep soil carbon decomposability but not deep soil nitrogen
863 dynamics. *Proceedings of the National Academy of Sciences*, 112(12), 3752–3757.
864 <https://doi.org/10.1073/pnas.1415123112>
- 865 Koyama, A., Wallenstein, M. D., Simpson, R. T., & Moore, J. C. (2013). Carbon-
866 Degrading Enzyme Activities Stimulated by Increased Nutrient Availability in
867 Arctic Tundra Soils. *PLoS ONE*, 8(10).<https://doi.org/10.1371/journal.pone.0077212>
- 868 Kwon, M. J., Heimann, M., Kolle, O., Luus, K. A., Schuur, E. A., Zimov, N., ... &
869 Göckede, M. (2016). Long-term drainage reduces CO₂ uptake and increases CO₂
870 emission on a Siberian floodplain due to shifts in vegetation community and soil
871 thermal characteristics. *Biogeosciences*, 13(14), 4219–4235.
872 <https://doi.org/10.5194/bg-13-4219-2016>
- 873 Kuznetsova A., Brockhoff P. B. and Christensen R. H. B. (2017). lmerTest Package:
874 Tests in Linear Mixed Effects Models. *Journal of Statistical Software*, 82(13), 1–26.
875 <https://doi.org/10.18637/jss.v082.i13>
- 876 Lefebvre, J., Gauthier, G., Giroux, J. F., Reed, A., Reed, E. T., & Bélanger, L. (2017).
877 The greater snow goose *Anser caerulescens atlanticus*: Managing an overabundant
878 population. *Ambio*, 46(2), 262–274. <https://doi.org/10.1007/s13280-016-0887-1>
- 879 Leffler, A. J., Klein, E. S., Oberbauer, S. F., & Welker, J. M. (2016). Coupled long-term
880 summer warming and deeper snow alters species composition and stimulates gross
881 primary productivity in tussock tundra. *Oecologia*, 181(1), 287–297.
882 <https://doi.org/10.1007/s00442-015-3543-8>
- 883 Lenth, R. V. (2021). *emmeans: Estimated Marginal Means, aka Least-Squares Means. R*
884 *package version 1.6.2-1*. Retrieved from [https://cran.r-](https://cran.r-project.org/package=emmeans)
885 [project.org/package=emmeans](https://cran.r-project.org/package=emmeans)
- 886 Liljedahl, A. K., Hinzman, L. D., Harazono, Y., Zona, D., Tweedie, C. E., Hollister, R.
887 D., ... & Oechel, W. C. (2011). Nonlinear controls on evapotranspiration in Arctic
888 coastal wetlands. *Biogeosciences*, 8(11), 3375–3389. [https://doi.org/10.5194/bg-8-](https://doi.org/10.5194/bg-8-3375-2011)
889 [3375-2011](https://doi.org/10.5194/bg-8-3375-2011)

- 890 Liu, N., Michelsen, A., & Rinnan, R. (2020). Vegetation and soil responses to added
891 carbon and nutrients remain six years after discontinuation of long-term treatments.
892 *Science of the Total Environment*, 722, 137885.
893 <https://doi.org/10.1016/j.scitotenv.2020.137885>
- 894 Mack, M. C., Schuur, E. A. G., Bret-Harte, M. S., Shaver, G. R., & Chapin III, F. S.
895 (2004). Ecosystem carbon storage in arctic tundra reduce by long-term nutrient
896 fertilization. *Nature*, 431(7007), 440–443. <https://doi.org/10.1038/nature02887>
- 897 Maclean, I. M. D., Mosedale, J. R., & Bennie, J. J. (2019). Microclima: An r package for
898 modelling meso- and microclimate. *Methods in Ecology and Evolution*, 10(2), 280–
899 290. <https://doi.org/10.1111/2041-210X.13093>
- 900 Mattheis, P. J., & Tieszen, L. L. (1976). Responses of *Dupontia fischeri* to Simulated
901 Lemming Grazing in an Alaskan Arctic Tundra. *Annals of Botany*, 40 (166), 179–
902 197. <https://doi.org/10.1093/oxfordjournals.aob.a085121>
- 903 McFadden, J. P., Chapin, F. S., & Hollinger, D. Y. (1998). Subgrid-scale variability in
904 the surface energy balance of arctic tundra. *Journal of Geophysical Research*
905 *Atmospheres*, 103(D22), 28947–28961. <https://doi.org/10.1029/98jd02400>
- 906 Miner, K. R., Turetsky, M. R., Malina, E., Bartsch, A., Tamminen, J., McGuire, A. D.,
907 Fix, A., Sweeney, C., Elder, C. D., & Miller, C. E. (2022). Permafrost carbon
908 emissions in a changing Arctic. *Nature Reviews Earth and Environment*, 3(1), 55–
909 67. <https://doi.org/10.1038/s43017-021-00230-3>
- 910 Mosbacher, J. B., Michelsen, A., Stelvig, M., Hjermstad-Sollerud, H., & Schmidt, N. M.
911 (2019). Muskoxen Modify Plant Abundance, Phenology, and Nitrogen Dynamics in
912 a High Arctic Fen. *Ecosystems*, 22(5), 1095–1107. [https://doi.org/10.1007/s10021-](https://doi.org/10.1007/s10021-018-0323-4)
913 [018-0323-4](https://doi.org/10.1007/s10021-018-0323-4)
- 914 Myers-Smith, I. H., Forbes, B. C., Wilking, M., Hallinger, M., Lantz, T., Blok, D., ...
915 Hik, D. S. (2011). Shrub expansion in tundra ecosystems: Dynamics, impacts and
916 research priorities. *Environmental Research Letters*, 6(4).
917 <https://doi.org/10.1088/1748-9326/6/4/045509>
- 918 Natali, S. M., Schuur, E. A. G., Trucco, C., Hicks Pries, C. E., Crummer, K. G., & Baron
919 Lopez, A. F. (2011). Effects of experimental warming of air, soil and permafrost on
920 carbon balance in Alaskan tundra. *Global Change Biology*, 17(3), 1394–1407.
921 <https://doi.org/10.1111/j.1365-2486.2010.02303.x>
- 922 Nishizawa, K., Deschamps, L., Maire, V., Bêty, J., Lévesque, E., Kitagawa, R.,
923 Masumoto, S., Gosselin, I., Morneau, A., Rochefort, L., Gauthier, G., Tanabe, Y.,
924 Uchida, M., & Mori, A. S. (2021). Long-term consequences of goose exclusion on
925 nutrient cycles and plant communities in the High-Arctic. *Polar Science*, 27
926 (December 2020). <https://doi.org/10.1016/j.polar.2020.100631>

- 927 Nowinski, N. S., Trumbore, S. E., Schuur, E. A. G., MacK, M. C., & Shaver, G. R.
928 (2008). Nutrient addition prompts rapid destabilization of organic matter in an arctic
929 tundra ecosystem. *Ecosystems*, 11(1), 16–25. [https://doi.org/10.1007/s10021-007-](https://doi.org/10.1007/s10021-007-9104-1)
930 [9104-1](https://doi.org/10.1007/s10021-007-9104-1)
- 931 O'Donnell, J. A., Romanovsky, V. E., Harden, J. W., & Mcguire, A. D. (2009). The
932 Effect of Moisture Content on the Thermal Conductivity of Moss and Organic Soil
933 Horizons from Black Spruce Ecosystems in Interior Alaska. *Soil Science*, 174 (12),
934 646–651. <https://doi.org/10.1097/SS.0b013e3181c4a7f8>
- 935 Ola, A., Fortier, D., Coulombe, S., Comte, J., & Domine, F. (2022). The Distribution of
936 Soil Carbon and Nitrogen Stocks Among Dominant Geomorphological Terrain
937 Units in Qarlikturvik Valley, Bylot Island, Arctic Canada. *Journal of Geophysical*
938 *Research: Biogeosciences*, 127(7). <https://doi.org/10.1029/2021JG006750>
- 939 Pouliot, R., Rochefort, L., & Gauthier, G. (2009). Moss carpets constrain the fertilizing
940 effects of herbivores on graminoid plants in arctic polygon fens. *Botany*, 87, 1209–
941 1222. <https://doi.org/10.1139/B09-069>
- 942 Prager, C. M., Naeem, S., Boelman, N. T., Eitel, J. U. H., Greaves, H. E., Heskell, M. A.,
943 ... & Griffin, K. L. (2017). A gradient of nutrient enrichment reveals nonlinear
944 impacts of fertilization on Arctic plant diversity and ecosystem function. *Ecology and*
945 *Evolution*, 7(7), 2449–2460. <https://doi.org/10.1002/ece3.2863>
- 946 Raillard, M. C., & Svoboda, J. (1999). Exact Growth and Increased Nitrogen
947 Compensation by the Arctic Sedge *Carex aquatilis* var. *stans* after Simulated Grazing.
948 *Arctic, Antarctic, and Alpine Research*, 31(1), 21–26.
949 <https://doi.org/10.1080/15230430.1999.12003277>
- 950 Reed, A., Hughes, R. J., & Boyd, H. (2002). Patterns of distribution and abundance of
951 Greater Snow Geese on Bylot Island, Nunavut, Canada 1983-1998. *Wildfowl*, 53,
952 53–65.
- 953 Schädel, C., Koven, C. D., Lawrence, D. M., Celis, G., Garnello, A. J., Hutchings, J.,
954 Mauritz, M., Natali, S. M., Pegoraro, E., Rodenhizer, H., Salmon, V. G., Taylor, M.
955 A., Webb, E. E., Wieder, W. R., & Schuur, E. A. (2018). Divergent patterns of
956 experimental and model-derived permafrost ecosystem carbon dynamics in response
957 to Arctic warming. *Environmental Research Letters*, 13 (10), 105002.
958 <https://doi.org/10.1088/1748-9326/aae0ff>
- 959 Schuur, E. A. G., Vogel, J. G., Crummer, K. G., Lee, H., Sickman, J. O., & Osterkamp,
960 T. E. (2009). The effect of permafrost thaw on old carbon release and net carbon
961 exchange from tundra. *Nature*, 459(7246), 556–559.
962 <https://doi.org/10.1038/nature08031>

- 963 Shaver, G. R., & Chapin, F. S. (1995). Long-term responses to factorial, NPK fertilizer
964 treatment by Alaskan wet and moist tundra sedge species. *Ecography*, *18*(3), 259–
965 275. <https://doi.org/10.1111/j.1600-0587.1995.tb00129.x>
- 966 Shaver, G. R., Syndergaard, M., Jones, M. H., Johnstone, J., Gough, L., Laundre,
967 J., & Stuart Chapin, F. (2001). Species composition interacts with fertilizer to
968 control long-term change in tundra productivity. *Ecology*, *82*(11), 3163–3181.
969 [https://doi.org/10.1890/0012-9658\(2001\)082\[3163:SCIWFT\]2.0.CO;2](https://doi.org/10.1890/0012-9658(2001)082[3163:SCIWFT]2.0.CO;2)
- 970 Shur, Y., Hinkel, K. M., & Nelson, F. E. (2005). The transient layer: Implications for
971 geocryology and climate-change science. *Permafrost and Periglacial Processes*,
972 *16*(1), 5–17. <https://doi.org/10.1002/ppp.518>
- 973 Sjögersten, S., van der Wal, R., Loonen, M. J. J. E., & Woodin, S. J. (2011). Recovery of
974 ecosystem carbon fluxes and storage from herbivory. *Biogeochemistry*, *106*(3), 357–
975 370. <https://doi.org/10.1007/s10533-010-9516-4>
- 976 Sjögersten, S., van der Wal, R., & Woodin, S. J. (2012). Impacts of Grazing and Climate
977 Warming on C Pools and Decomposition Rates in Arctic Environments. *Ecosystems*,
978 *15*(3), 349–362. <https://doi.org/10.1007/s10021-011-9514-y>
- 979 Soudzilovskaia, N. A., Bodegom, P. M. Van, & Cornelissen, J. H. C. (2013). Dominant
980 bryophyte control over high-latitude soil temperature fluctuations predicted by heat
981 transfer traits, field moisture regime and laws of thermal insulation. *Functional*
982 *Ecology*, *27*, 1442–1454. <https://doi.org/10.1111/1365-2435.12127>
- 983 Speed, J. D. M., Woodin, S. J., Tømmervik, H., & van der Wal, R. (2010). Extrapolating
984 herbivore-induced carbon loss across an arctic landscape. *Polar Biology*, *33*(6), 789–
985 797. <https://doi.org/10.1007/s00300-009-0756-5>
- 986 Sundqvist, M. K., Moen, J., Björk, R. G., Vowles, T., Kytöviita, M. M., Parsons, M. A.,
987 & Olofsson, J. (2019). Experimental evidence of the long-term effects of reindeer on
988 Arctic vegetation greenness and species richness at a larger landscape scale. *Journal*
989 *of Ecology*, *107*(6), 2724–2736. <https://doi.org/10.1111/1365-2745.13201>
- 990 te Beest, M., Sitters, J., Ménard, C. B., & Olofsson, J. (2016). Reindeer grazing increases
991 summer albedo by reducing shrub abundance in Arctic tundra. *Environmental*
992 *Research Letters*, *11*(12). <https://doi.org/10.1088/1748-9326/aa5128>
- 993 R Core Team (2020). *R: A language and environment for statistical computing*. Vienna,
994 Austria: R Foundation for Statistical Computing. Retrieved from [https://www.r-](https://www.r-project.org/)
995 [project.org/](https://www.r-project.org/).
- 996 Valéry, L., Cadieux, M. C., & Gauthier, G. (2010). Spatial heterogeneity of primary
997 production as both cause and consequence of foraging patterns of an expanding

- 998 greater snow goose colony. *Ecoscience*, 17(1), 9–19. [https://doi.org/10.2980/17-1-](https://doi.org/10.2980/17-1-3279)
999 3279
- 1000 van der Wal, R., Van Lieshout, S. M. J., & Loonen, M. J. J. E. (2001). Herbivore impact
1001 on moss depth, soil temperature and arctic plant growth. *Polar Biology*, 24(1), 29–
1002 32. <https://doi.org/10.1007/s003000000170>
- 1003 van der Wal, R., Sjögersten, S., Woodin, S. J., Cooper, E. J., Jónsdóttir, I. S., Kuijper,
1004 D., ... & Huiskes, A. D. (2007). Spring feeding by pink-footed geese reduces carbon
1005 stocks and sink strength in tundra ecosystems. *Global Change Biology*, 13(2), 539–
1006 545. <https://doi.org/10.1111/j.1365-2486.2006.01310.x>
- 1007 van Wijk, M. T., Clemmensen, K. E., Shaver, G. R., Williams, M., Callaghan, T. V.,
1008 Chapin, F. S., ... & Rueth, H. (2004). Long-term ecosystem level experiments at
1009 Toolik Lake, Alaska, and at Abisko, Northern Sweden: Generalizations and
1010 differences in ecosystem and plant type responses to global change. *Global Change*
1011 *Biology*, 10(1), 105–123. <https://doi.org/10.1111/j.1365-2486.2003.00719.x>
- 1012 Vincent, W. F., Lemay, M., & Allard, M. (2017). Arctic permafrost landscapes in
1013 transition: towards an integrated Earth system approach. *Arctic Science*, 3(2), 39–64.
1014 <https://doi.org/10.1139/as-2016-0027>
- 1015 Voigt, C., Lamprecht, R. E., Marushchak, M. E., Lind, S. E., Novakovskiy, A., Aurela,
1016 M., ... & Biasi, C. (2017). Warming of subarctic tundra increases emissions of all
1017 three important greenhouse gases – carbon dioxide, methane, and nitrous oxide.
1018 *Global Change Biology*, 23(8), 3121–3138. <https://doi.org/10.1111/gcb.13563>
- 1019 Wang, P., Limpens, J., Mommer, L., van Ruijven, J., Nauta, A. L., Berendse, F., ... &
1020 Heijmans, M. M. P. D. (2017). Above- and below-ground responses of four tundra
1021 plant functional types to deep soil heating and surface soil fertilization. *Journal of*
1022 *Ecology*, 105(4), 947–957. <https://doi.org/10.1111/1365-2745.12718>
- 1023 Wood, S. N. (2011). Fast stable restricted maximum likelihood and marginal likelihood
1024 estimation of semiparametric generalized linear models. *Journal of the Royal*
1025 *Statistical Society: Series B (Statistical Methodology)*, 73(1), 3–36.
1026 <https://doi.org/10.1111/j.1467-9868.2010.00749.x>
- 1027 Yi, S., Woo, M. K., & Arain, M. A. (2007). Impacts of peat and vegetation on permafrost
1028 degradation under climate warming. *Geophysical Research Letters*, 34(16), 1–5.
1029 <https://doi.org/10.1029/2007GL030550>
- 1030 Yläne, H., Kaarlejärvi, E., Väisänen, M., Männistö, M. K., Ahonen, S. H. K., Olofsson,
1031 J., & Stark, S. (2020). Removal of grazers alters the response of tundra soil carbon
1032 to warming and enhanced nitrogen availability. *Ecological Monographs*, 90(1), 1–
1033 13. <https://doi.org/10.1002/ecm.1396>

- 1034 Zhu, D., Ciais, P., Krinner, G., Maignan, F., Jornet Puig, A., & Hugelius, G. (2019).
1035 Controls of soil organic matter on soil thermal dynamics in the northern high
1036 latitudes. *Nature Communications*, 10(1), 1–9. [https://doi.org/10.1038/s41467-019-](https://doi.org/10.1038/s41467-019-11103-1)
1037 11103-1
- 1038 Zoltai, S. C., & McCormick, K. J. (1983). A natural resource survey of Bylot Island
1039 and adjacent Baffin Island, Northwest Territories. Parks Canada, Ottawa, Ontario,
1040 Canada